

The ANTs longitudinal cortical thickness pipeline

Nicholas J. Tustison^{1,2}, Andrew J. Holbrook³, Jared M. Roberts², Brian B. Avants⁴, James R. Stone¹, Daniel L. Gillen³, and Michael A. Yassa² for the Alzheimer's Disease Neuroimaging Initiative*

¹Department of Radiology and Medical Imaging, University of Virginia, Charlottesville, VA

²Department of Neurobiology and Behavior, University of California, Irvine, Irvine, CA

³Department of Statistics, University of California, Irvine, Irvine, CA

⁴ Biogen, Cambridge, MA

Corresponding author:

Nicholas J. Tustison

4173 Cardamon Circle

Corona, CA 92883

540-383-2719

ntustison@virginia.edu

*Data used in preparation of this article were obtained from the Alzheimer's Disease Neuroimaging Initiative (ADNI) database (adni.loni.usc.edu). As such, the investigators within the ADNI contributed to the design and implementation of ADNI and/or provided data but did not participate in analysis or writing of this report. A complete listing of ADNI investigators can be found at: http://adni.loni.usc.edu/wp-content/uploads/how_to_apply/ADNI_Acknowledgement_List.pdf

Notes for discussion

- change the title?

Abstract

Large-scale longitudinal studies of disease and pathology in the human brain have motivated the acquisition of large neuroimaging data sets and the concomitant development of robust methodological and statistical tools for insight into potential neurostructural changes. Longitudinal strategies for acquisition and processing have potentially significant benefits including the reduction of the inter-subject variability of corresponding cross-sectional studies. In this work, we introduce the open-source Advanced Normalization Tools (ANTs) cortical thickness longitudinal processing pipeline and its application on the Alzheimer's Disease Neuroimaging Initiative 1 data set consisting of over 600 subjects with multiple time points from baseline to 36 months. We show that single-subject template construction and native subject-space processing localizes data transformations and reduces interpolation artifacts, respectively, and is the preferred strategy for minimizing within-subject variability and maximizing between-subject variability. Furthermore, we demonstrate that these criteria lead to greater diagnostic predictive accuracy over other possible processing strategies. In the spirit of open-science, the ANTs software (including the longitudinal cortical thickness processing framework), regional data tables, and processing scripts are publicly available.

Introduction

Quantification of brain morphology has proven invaluable in studying conditional abnormalities such as Huntington's disease [1–3], schizophrenia [4], bipolar disorder [5], Alzheimer's disease and frontotemporal dementia [6], Parkinson's disease [8], Williams syndrome [9], multiple sclerosis [10], autism [11], migraines [13], chronic smoking [14], alcoholism [15], cocaine addiction [16], marijuana use in adolescents [17], Tourette syndrome in children [18], scoliosis in female adolescents [19], heart failure [20], early-onset blindness [21], chronic pancreatitis [22], obsessive-compulsive disorder [23], ADHD [24], obesity [25], and heritable [26] and elderly [27] depression. Evidence of cortical thickness variation has also been found to be a function of age [28], gender [29], untreated male-to-female transsexuality [30], handedness [31], intelligence [32], athletic ability [33], meditative practices [34], musical ability [35], musical instrument playing [37], tendency toward criminality [38], childhood sexual abuse in adult females [39], and Tetris-playing ability in female adolescents [40]. Additionally, connectivity studies demonstrate structural relationships using cortical thickness measures [41].

Large neuroimaging datasets such as those provided by the Alzheimer's Disease Neuroimaging Initiative (ADNI) are increasing the importance of fully automated and multiple modality brain mapping tools [42]. The scale of such datasets will only increase over time as international projects continue to build large-scale neuroimaging data resources. Currently, the National Institutes of Health (NIH) also mandates that any NIH-funded data resources, including MRI, must be released to the public. In contrast to ADNI, which provides standardized data acquisition protocols used across all sites, these smaller-scale projects are collected in an unstructured way. Therefore, neuroimage processing tools must reliably quantify even when there is a relative lack of quality control over the input data. While robustness is a goal shared by all software development targeted at neuroscience, very few methods have been thoroughly tested on large and unstructured neuroimaging datasets.

Materials and Methods

Imaging

Cortical thickness

Single time point processing

In [43] we introduced the ANTs cortical thickness processing pipeline using a large cohort of ~ 1200 images taken from four popular, publicly available data sets with ages ranging from 4 to 97 years. The processing pipeline comprises the following four major steps (cf Figure 1 of [43]):

- N4 bias correction [44],
- brain extraction [45],
- Atropos six-tissue segmentation [46], and
- cortical thickness estimation [47]

which is enhanced by the use of optimal shape and intensity templates derived from the specific populations of study. Regional statistics were quantified by parcellating the cortex using a collection of 20 atlases from the OASIS test-retest data which were labeled using the Desikan-Killiany-Tourville (DKT) protocol [48] consisting of 31 labels per hemisphere (see Table 1). Consensus labelings in each subject were generated from the joint label fusion approach of [49]. A thickness-based evaluation with the well-known FreeSurfer algorithm demonstrated better predictive performance of age and gender. Since the original publication, we have added multi-modal capabilities and the optional inclusion of patch-based denoising based on an ANTs implementation of the patch-based denoising algorithm of [50]. The resulting regional statistics (including cortical thickness, surface area [51], volumes, and Jacobian determinant values) were posted online (<https://github.com/ntustison/KapowskiChronicles>). These include the corresponding FreeSurfer measurements which are also publicly available for research studies (e.g., [52]). Since publication, this pipeline has been used in a number of cross-sectional studies [53–55].

Table 1: The 31 cortical labels (per hemisphere) of the Desikan-Killiany-Tourville atlas. The ROI abbreviations from the R brainGraph package are given and used in later figures.

1) caudal anterior cingulate (cACC)	17) pars orbitalis (pORB)
2) caudal middle frontal (cMFG)	18) pars triangularis (pTRI)
3) cuneus (CUN)	19) pericalcarine (periCAL)
4) entorhinal (ENT)	20) postcentral (postC)
5) fusiform (FUS)	21) posterior cingulate (PCC)
6) inferior parietal (IPL)	22) precentral (preC)
7) inferior temporal (ITG)	23) precuneus (PCUN)
8) isthmus cingulate (iCC)	24) rostral anterior cingulate (rACC)
9) lateral occipital (LOG)	25) rostral middle frontal (rMFG)
10) lateral orbitofrontal (LOF)	26) superior frontal (SFG)
11) lingual (LING)	27) superior parietal (SPL)
12) medial orbitofrontal (MOF)	28) superior temporal (STG)
13) middle temporal (MTG)	29) supramarginal (SMAR)
14) parahippocampal (PARH)	30) transverse temporal (TT)
15) paracentral (paraC)	31) insula (INS)
16) pars opercularis (pOPER)	

Unbiased longitudinal processing

Overview. See Figure 1. The ANTs longitudinal cortical thickness pipeline extends the ANTs cortical thickness pipeline for longitudinal studies which takes into account various bias issues which have been discussed in the literature [57]. Prior to the processing of any individual subjects a group template [60] and corresponding auxiliary images (i.e., six-tissue and brain extraction prior probability maps) are generated. This cohort is typically composed of a subset of the study subjects.

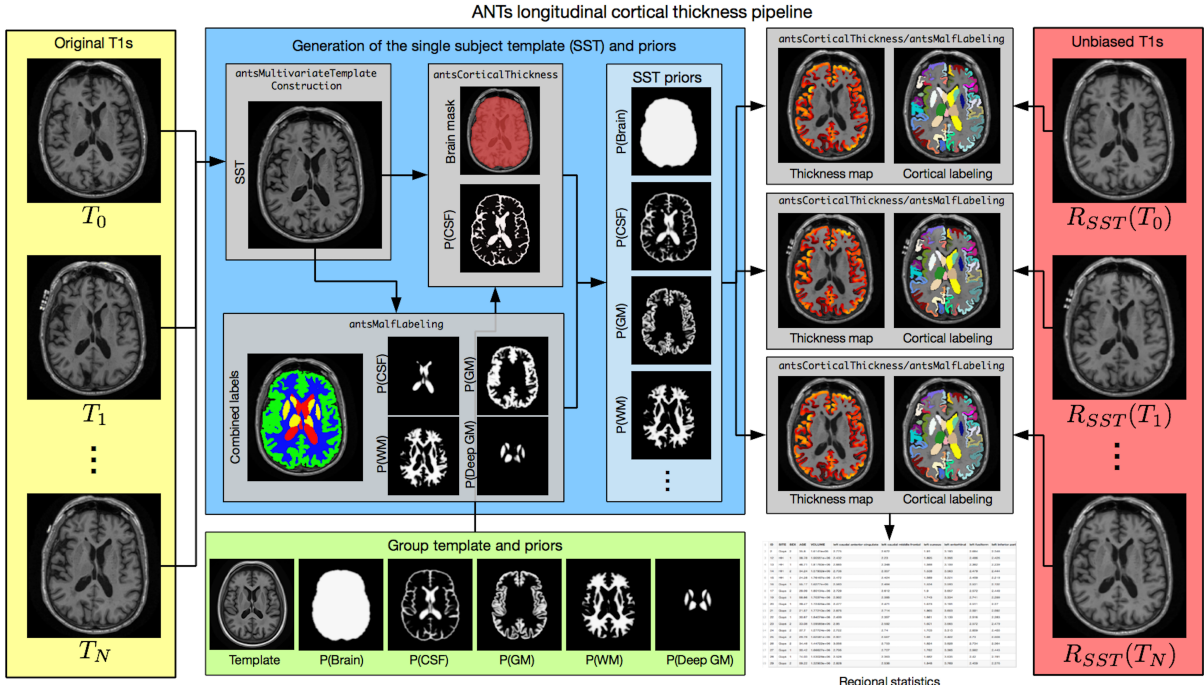


Figure 1: The ANTs longitudinal cortical thickness pipeline. The original T1-weighted images are used to generate an unbiased single-subject template (SST). The SST is then processed via the segmentation portion of the ANTs cross-sectional cortical thickness pipeline reported in [56] using the group template and tissue priors. This results in a probabilistic estimate of the CSF and the brain mask. Joint label fusion (JLF) of 20 atlases involving six labels (CSF, gray matter, white matter, deep gray matter, brain stem, and cerebellum) is used to get a probabilistic estimate of the six tissues. The latter five JLF probabilistic tissue estimates are used as the SST prior probabilities whereas the CSF SST prior probability is derived as a combination of the JLF and segmentation CSF estimates, i.e., $P(CSF) = \max(P_{Seg}(CSF), P_{JLF}(CSF))$. The T1-weighted image at each time point is rigidly aligned to the template and processed through original cortical thickness pipeline using the SST template and auxiliary images (brain extraction mask and tissue priors). Cortical labelings obtained using JLF are then used to quantify ROI-based statistics.

Following the offline construction of the group template and prior probability images, each subject undergoes similar processing. First, an average shape and intensity single subject template (SST) is created from all time point images [60]. Each time point image is then rigidly aligned to the SST. The SST prior probability maps are created using a protocol combining brain extraction and a six-tissue segmentation and a six-label joint label fusion processing of the SST. After the SST template priors are created, each time point image is rigidly aligned to the template to reduce the effect of coordinate system or interpolation bias.

Each rigidly-aligned time point image is processed using the ANTs original pipeline and the SST template and template priors resulting in a brain extraction mask, six-tissue segmentation, and a cortical thickness map for each time point image. The cortical ROIs from the DKT atlases are propagated to each time point using a “pseudo-geodesic” mapping and joint label fusion.

Subsequent processing segments the SST into six probabilistic tissue classes: cerebrospinal fluid (CSF), gray matter (GM), white matter (WM), deep gray matter (striatum + thalamus), brain stem, and cerebellum. This requires processing the SST through two parallel workflows. First, the SST proceeds through the standard ANTs cortical thickness pipeline which generates a brain extraction mask and the CSF posterior probability map. Second, using a data set of expert annotations [48], a class-leading multi-atlas joint label fusion step [49] is performed to create individualized probability maps for all tissue types. This final version of the SST enables unbiased mappings to the group template, subject-specific tissue segmentations, region of interest volumes and cortical thickness maps for each of the original time series images. The corresponding cortical labelings (generated using a multi-atlas label fusion approach and a selected cortical parcellation protocol) are then used to tabulate regional thickness and area values for statistical analysis. Other modalities are then mapped to the group template through these unbiased transformations, as in [56, 61]

ADNI normal template.

“Cooking” the template priors.

Pseudo-geodesic for large cohort labeling.

Notes to self:

- Add an image and discussion of the pseudo-geodesic for facilitating multi-labeling.
- Discuss the ants implementation (multi-threading, etc.)
- Discuss ADNI template

Statistical methods

We used a simple statistical principle to compare performance between cross-sectional and longitudinal processing methods. We said that one method outperforms the other when it does a better job minimizing within-subject variability and maximizing between-subject variability in cortical thickness measurements. Such a quality implies greater within-subject reproducibility while distinguishing between patient subpopulations. As such this will amount to higher precision when cortical thickness is used as a predictor variable or model covariate in statistical analyses upstream. This criterion is immediately assessable in terms of estimates associated to the longitudinal mixed-effects model outlined below.

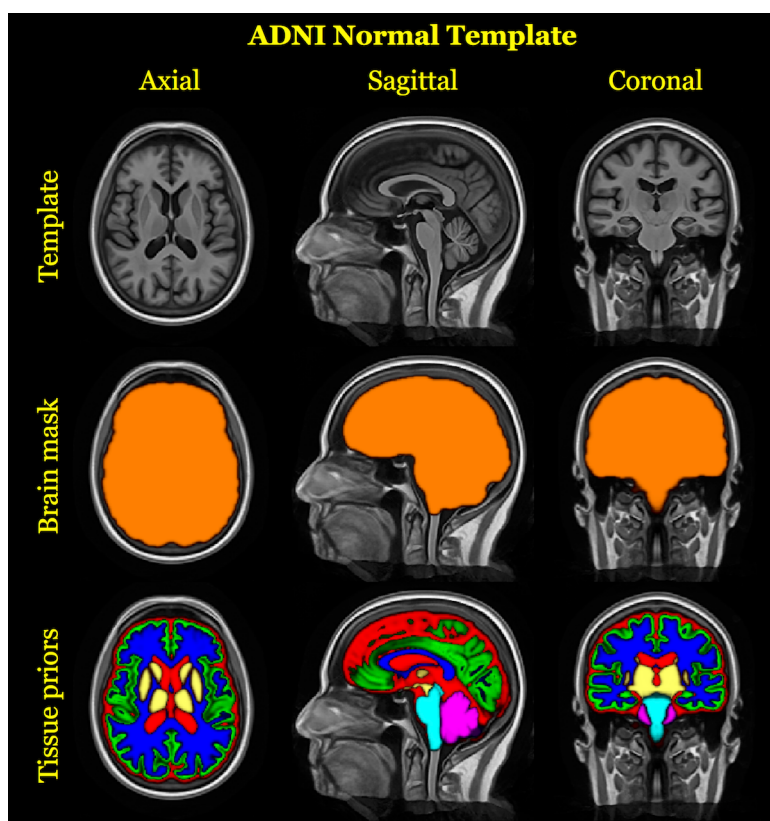


Figure 2: The ADNI normal template

As previously noted we observed yearly cortical thickness measurements from sixty-two separate regions of interest. To assess the above variance criterion while accounting for changes that may occur through the passage of time, we used a hierarchical Bayesian model for parameter estimation. Let Y_{ij}^k denote the i^{th} individual's cortical thickness measurement corresponding to the k^{th} region of interest at measurement j . Under the Bayesian paradigm we utilized a model of the form

$$\begin{aligned} Y_{ij}^k &\sim N(\alpha_i^k + \beta^k t, \sigma_k^2) \\ \alpha_i^k &\sim N(\alpha_0^k, \tau_k^2) \quad \alpha_0^k, \beta^k \sim N(0, 10) \quad \sigma_k^2, \tau_k^2 \sim \text{Cauchy}^+(0, 5) \end{aligned} \quad (1)$$

Specification of parameters in the above prior distributions reflect commonly accepted diffuse priors. τ_k^2 represents the between-subject variance parameter, and σ_k^2 represents the within-subject variance parameter. For each region, the quantity of interest is thus the ratio $r^k = \frac{\tau_k^2}{\sigma_k^2}$. This ratio is closely related to the intraclass correlation coefficient [62]. The posterior distribution of r^k was summarized via the posterior median. Where the posterior distributions were obtained using Stan probabilistic programming language [63].

For each processing method we performed sixty-two independent regressions. In order to compare results between methods, we considered the quantity $\delta^k = r_l^k - r_c^k$ and $\delta_{norm}^k = \frac{r_l^k - r_c^k}{r_l^k + r_c^k}$, denoting the variance ratio for the longitudinal method minus that of the cross-sectional method and the normed difference between ratios, respectively (cf Figure ??). Since a large r^k implies a higher between-subject to within-subject variability ratio, a positive estimate of δ^k that is large in magnitude implies that the longitudinal processing method is preferable to the cross-sectional method. Conversely, a negative estimate that is large in magnitude implies that the cross-sectional processing method is preferable to the longitudinal method.

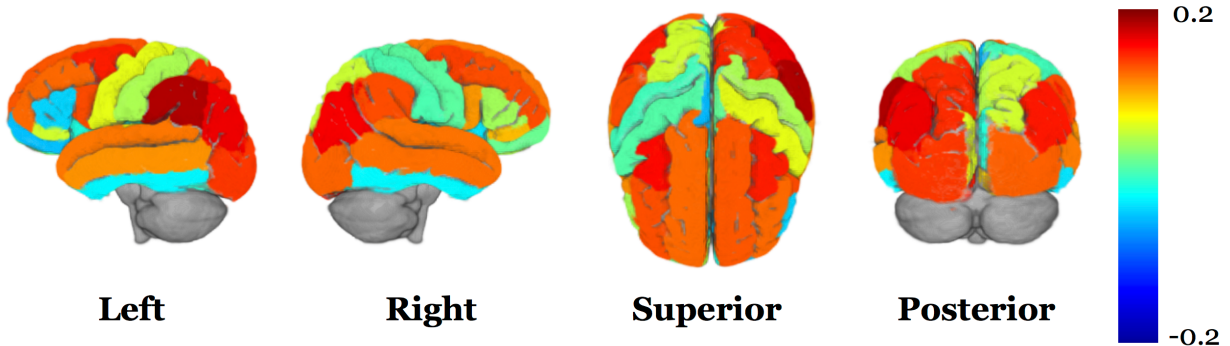


Figure 3: 3-D volumetric rendering of the normed difference of the longitudinal variance ratio minus the cross-sectional variance ratio specified for each of the 62 cortical regions.

Results

Discussion

Subsection 1

And a sweet equation:

$$\exp^{-i\pi} = -1$$

References

1. Rosas, H. D., Liu, A. K., Hersch, S., Glessner, M., Ferrante, R. J., Salat, D. H., Kouwe, A. van der, Jenkins, B. G., Dale, A. M., and Fischl, B. “**Regional and Progressive Thinning of the Cortical Ribbon in Huntington’s Disease**” *Neurology* 58, no. 5 (2002): 695–701.
2. Rosas, H. D., Hevelone, N. D., Zaleta, A. K., Greve, D. N., Salat, D. H., and Fischl, B. “**Regional Cortical Thinning in Preclinical Huntington Disease and Its Relationship to Cognition**” *Neurology* 65, no. 5 (2005): 745–7. doi:[10.1212/01.wnl.0000174432.87383.87](https://doi.org/10.1212/01.wnl.0000174432.87383.87)
3. Selemón, L. D., Rajkowska, G., and Goldman-Rakic, P. S. “**Evidence for Progression in Frontal Cortical Pathology in Late-Stage Huntington’s Disease**” *J Comp Neurol* 468, no. 2 (2004): 190–204. doi:[10.1002/cne.10938](https://doi.org/10.1002/cne.10938)
4. Nesvåg, R., Lawyer, G., Varnäs, K., Fjell, A. M., Walhovd, K. B., Frigessi, A., Jönsson, E. G., and Agartz, I. “**Regional Thinning of the Cerebral Cortex in Schizophrenia: Effects of Diagnosis, Age and Antipsychotic Medication**” *Schizophr Res* 98, no. 1-3 (2008): 16–28. doi:[10.1016/j.schres.2007.09.015](https://doi.org/10.1016/j.schres.2007.09.015)
5. Lyoo, I. K., Sung, Y. H., Dager, S. R., Friedman, S. D., Lee, J.-Y., Kim, S. J., Kim, N., Dunner, D. L., and Renshaw, P. F. “**Regional Cerebral Cortical Thinning in Bipolar Disorder**” *Bipolar Disord* 8, no. 1 (2006): 65–74. doi:[10.1111/j.1399-5618.2006.00284.x](https://doi.org/10.1111/j.1399-5618.2006.00284.x)
6. Du, A.-T., Schuff, N., Kramer, J. H., Rosen, H. J., Gorno-Tempini, M. L., Rankin, K., Miller, B. L., and Weiner, M. W. “**Different Regional Patterns of Cortical Thinning in Alzheimer’s Disease and Frontotemporal Dementia**” *Brain* 130, no. Pt 4 (2007): 1159–66. doi:[10.1093/brain/awm016](https://doi.org/10.1093/brain/awm016)
7. Dickerson, B. C., Bakkour, A., Salat, D. H., Feczko, E., Pacheco, J., Greve, D. N., Grodstein, F., Wright, C. I., Blacker, D., Rosas, H. D., Sperling, R. A., Atri, A., Growdon, J. H., Hyman, B. T., Morris, J. C., Fischl, B., and Buckner, R. L. “**The Cortical Signature of Alzheimer’s Disease: Regionally Specific Cortical Thinning Relates to Symptom Severity in Very Mild to Mild AD Dementia and Is Detectable in Asymptomatic Amyloid-Positive Individuals**” *Cereb Cortex* 19, no. 3 (2009): 497–510. doi:[10.1093/cercor/bhn113](https://doi.org/10.1093/cercor/bhn113)
8. Jubault, T., Gagnon, J.-F., Karama, S., Ptito, A., Lafontaine, A.-L., Evans, A. C., and Monchi, O. “**Patterns of Cortical Thickness and Surface Area in Early Parkinson’s Disease**” *Neuroimage* 55, no. 2 (2011): 462–7. doi:[10.1016/j.neuroimage.2010.12.043](https://doi.org/10.1016/j.neuroimage.2010.12.043)
9. Thompson, P. M., Lee, A. D., Dutton, R. A., Geaga, J. A., Hayashi, K. M., Eckert, M. A., Bellugi, U., Galaburda, A. M., Korenberg, J. R., Mills, D. L., Toga, A. W., and Reiss, A. L. “**Abnormal Cortical Complexity and Thickness Profiles Mapped in Williams Syndrome**” *J Neurosci* 25, no. 16 (2005): 4146–58. doi:[10.1523/JNEUROSCI.0165-05.2005](https://doi.org/10.1523/JNEUROSCI.0165-05.2005)
10. Ramasamy, D. P., Benedict, R. H. B., Cox, J. L., Fritz, D., Abdelrahman, N., Hussein, S., Minagar, A., Dwyer, M. G., and Zivadinov, R. “**Extent of Cerebellum, Subcortical and Cortical Atrophy in Patients with MS: A Case-Control Study**” *J Neurol Sci* 282, no. 1-2 (2009): 47–54. doi:[10.1016/j.jns.2008.12.034](https://doi.org/10.1016/j.jns.2008.12.034)
11. Chung, M. K., Robbins, S. M., Dalton, K. M., Davidson, R. J., Alexander, A. L., and Evans, A. C. “**Cortical**

Thickness Analysis in Autism with Heat Kernel Smoothing" *Neuroimage* 25, no. 4 (2005): 1256–65.
doi:[10.1016/j.neuroimage.2004.12.052](https://doi.org/10.1016/j.neuroimage.2004.12.052)

12. Hardan, A. Y., Muddasani, S., Vemulapalli, M., Keshavan, M. S., and Minshew, N. J. "An MRI Study of Increased Cortical Thickness in Autism" *Am J Psychiatry* 163, no. 7 (2006): 1290–2.
doi:[10.1176/appi.ajp.163.7.1290](https://doi.org/10.1176/appi.ajp.163.7.1290)

13. DaSilva, A. F. M., Granziera, C., Snyder, J., and Hadjikhani, N. "Thickening in the Somatosensory Cortex of Patients with Migraine" *Neurology* 69, no. 21 (2007): 1990–5. doi:[10.1212/01.wnl.0000291618.32247.2d](https://doi.org/10.1212/01.wnl.0000291618.32247.2d)

14. Kühn, S., Schubert, F., and Gallinat, J. "Reduced Thickness of Medial Orbitofrontal Cortex in Smokers" *Biol Psychiatry* 68, no. 11 (2010): 1061–5. doi:[10.1016/j.biopsych.2010.08.004](https://doi.org/10.1016/j.biopsych.2010.08.004)

15. Fortier, C. B., Leritz, E. C., Salat, D. H., Venne, J. R., Maksimovskiy, A. L., Williams, V., Milberg, W. P., and McGlinchey, R. E. "Reduced Cortical Thickness in Abstinent Alcoholics and Association with Alcoholic Behavior" *Alcohol Clin Exp Res* 35, no. 12 (2011): 2193–201. doi:[10.1111/j.1530-0277.2011.01576.x](https://doi.org/10.1111/j.1530-0277.2011.01576.x)

16. Makris, N., Gasic, G. P., Kennedy, D. N., Hodge, S. M., Kaiser, J. R., Lee, M. J., Kim, B. W., Blood, A. J., Evins, A. E., Seidman, L. J., Iosifescu, D. V., Lee, S., Baxter, C., Perlis, R. H., Smoller, J. W., Fava, M., and Breiter, H. C. "Cortical Thickness Abnormalities in Cocaine Addiction—a Reflection of Both Drug Use and a Pre-Existing Disposition to Drug Abuse?" *Neuron* 60, no. 1 (2008): 174–88.
doi:[10.1016/j.neuron.2008.08.011](https://doi.org/10.1016/j.neuron.2008.08.011)

17. Jacobus, J., Squeglia, L. M., Meruelo, A. D., Castro, N., Brumback, T., Giedd, J. N., and Tapert, S. F. "Cortical Thickness in Adolescent Marijuana and Alcohol Users: A Three-Year Prospective Study from Adolescence to Young Adulthood" *Dev Cogn Neurosci* 16, (2015): 101–9.
doi:[10.1016/j.dcn.2015.04.006](https://doi.org/10.1016/j.dcn.2015.04.006)

18. Sowell, E. R., Kan, E., Yoshii, J., Thompson, P. M., Bansal, R., Xu, D., Toga, A. W., and Peterson, B. S. "Thinning of Sensorimotor Cortices in Children with Tourette Syndrome" *Nat Neurosci* 11, no. 6 (2008): 637–9. doi:[10.1038/nn.2121](https://doi.org/10.1038/nn.2121)

19. Wang, D., Shi, L., Chu, W. C. W., Burwell, R. G., Cheng, J. C. Y., and Ahuja, A. T. "Abnormal Cerebral Cortical Thinning Pattern in Adolescent Girls with Idiopathic Scoliosis" *Neuroimage* 59, no. 2 (2012): 935–42. doi:[10.1016/j.neuroimage.2011.07.097](https://doi.org/10.1016/j.neuroimage.2011.07.097)

20. Kumar, R., Yadav, S. K., Palomares, J. A., Park, B., Joshi, S. H., Ogren, J. A., Macey, P. M., Fonarow, G. C., Harper, R. M., and Woo, M. A. "Reduced Regional Brain Cortical Thickness in Patients with Heart Failure" *PLoS One* 10, no. 5 (2015): e0126595. doi:[10.1371/journal.pone.0126595](https://doi.org/10.1371/journal.pone.0126595)

21. Jiang, J., Zhu, W., Shi, F., Liu, Y., Li, J., Qin, W., Li, K., Yu, C., and Jiang, T. "Thick Visual Cortex in the Early Blind" *J Neurosci* 29, no. 7 (2009): 2205–11. doi:[10.1523/JNEUROSCI.5451-08.2009](https://doi.org/10.1523/JNEUROSCI.5451-08.2009)

22. Frøkjær, J. B., Bouwense, S. A. W., Olesen, S. S., Lundager, F. H., Eskildsen, S. F., Goor, H. van, Wilder-Smith, O. H. G., and Drewes, A. M. "Reduced Cortical Thickness of Brain Areas Involved in Pain Processing in Patients with Chronic Pancreatitis" *Clin Gastroenterol Hepatol* 10, no. 4 (2012): 434–

8.e1. doi:[10.1016/j.cgh.2011.11.024](https://doi.org/10.1016/j.cgh.2011.11.024)

23. Shin, Y.-W., Yoo, S. Y., Lee, J. K., Ha, T. H., Lee, K. J., Lee, J. M., Kim, I. Y., Kim, S. I., and Kwon, J. S. **“Cortical Thinning in Obsessive Compulsive Disorder”** *Hum Brain Mapp* 28, no. 11 (2007): 1128–35. doi:[10.1002/hbm.20338](https://doi.org/10.1002/hbm.20338)
24. Almeida Montes, L. G., Prado Alcántara, H., Martínez García, R. B., De La Torre, L. B., Avila Acosta, D., and Duarte, M. G. **“Brain Cortical Thickness in ADHD: Age, Sex, and Clinical Correlations”** *J Atten Disord* (2012): doi:[10.1177/1087054711434351](https://doi.org/10.1177/1087054711434351)
25. Raji, C. A., Ho, A. J., Parikshak, N. N., Becker, J. T., Lopez, O. L., Kuller, L. H., Hua, X., Leow, A. D., Toga, A. W., and Thompson, P. M. **“Brain Structure and Obesity”** *Hum Brain Mapp* 31, no. 3 (2010): 353–64. doi:[10.1002/hbm.20870](https://doi.org/10.1002/hbm.20870)
26. Peterson, B. S., Warner, V., Bansal, R., Zhu, H., Hao, X., Liu, J., Durkin, K., Adams, P. B., Wickramaratne, P., and Weissman, M. M. **“Cortical Thinning in Persons at Increased Familial Risk for Major Depression”** *Proc Natl Acad Sci U S A* 106, no. 15 (2009): 6273–8. doi:[10.1073/pnas.0805311106](https://doi.org/10.1073/pnas.0805311106)
27. Ballmaier, M., Sowell, E. R., Thompson, P. M., Kumar, A., Narr, K. L., Lavretsky, H., Welcome, S. E., DeLuca, H., and Toga, A. W. **“Mapping Brain Size and Cortical Gray Matter Changes in Elderly Depression”** *Biol Psychiatry* 55, no. 4 (2004): 382–9. doi:[10.1016/j.biopsych.2003.09.004](https://doi.org/10.1016/j.biopsych.2003.09.004)
28. Kochunov, P., Glahn, D. C., Lancaster, J., Thompson, P. M., Kochunov, V., Rogers, B., Fox, P., Blangero, J., and Williamson, D. E. **“Fractional Anisotropy of Cerebral White Matter and Thickness of Cortical Gray Matter Across the Lifespan”** *Neuroimage* 58, no. 1 (2011): 41–9. doi:[10.1016/j.neuroimage.2011.05.050](https://doi.org/10.1016/j.neuroimage.2011.05.050)
29. Luders, E., Narr, K. L., Thompson, P. M., Rex, D. E., Woods, R. P., Deluca, H., Jancke, L., and Toga, A. W. **“Gender Effects on Cortical Thickness and the Influence of Scaling”** *Hum Brain Mapp* 27, no. 4 (2006): 314–24. doi:[10.1002/hbm.20187](https://doi.org/10.1002/hbm.20187)
30. Luders, E., Sánchez, F. J., Tosun, D., Shattuck, D. W., Gaser, C., Vilain, E., and Toga, A. W. **“Increased Cortical Thickness in Male-to-Female Transsexualism”** *J Behav Brain Sci* 2, no. 3 (2012): 357–362. doi:[10.4236/jbbs.2012.23040](https://doi.org/10.4236/jbbs.2012.23040)
31. Luders, E., Narr, K. L., Thompson, P. M., Rex, D. E., Jancke, L., and Toga, A. W. **“Hemispheric Asymmetries in Cortical Thickness”** *Cereb Cortex* 16, no. 8 (2006): 1232–8. doi:[10.1093/cercor/bhj064](https://doi.org/10.1093/cercor/bhj064)
32. Shaw, P., Greenstein, D., Lerch, J., Clasen, L., Lenroot, R., Gogtay, N., Evans, A., Rapoport, J., and Giedd, J. **“Intellectual Ability and Cortical Development in Children and Adolescents”** *Nature* 440, no. 7084 (2006): 676–9. doi:[10.1038/nature04513](https://doi.org/10.1038/nature04513)
33. Wei, G., Zhang, Y., Jiang, T., and Luo, J. **“Increased Cortical Thickness in Sports Experts: A Comparison of Diving Players with the Controls”** *PLoS One* 6, no. 2 (2011): e17112. doi:[10.1371/journal.pone.0017112](https://doi.org/10.1371/journal.pone.0017112)
34. Lazar, S. W., Kerr, C. E., Wasserman, R. H., Gray, J. R., Greve, D. N., Treadway, M. T., McGarvey, M., Quinn, B. T., Dusek, J. A., Benson, H., Rauch, S. L., Moore, C. I., and Fischl, B. **“Meditation Experience Is**

- Associated with Increased Cortical Thickness”** *Neuroreport* 16, no. 17 (2005): 1893–7.
35. Bermudez, P., Lerch, J. P., Evans, A. C., and Zatorre, R. J. **“Neuroanatomical Correlates of Musicianship as Revealed by Cortical Thickness and Voxel-Based Morphometry”** *Cereb Cortex* 19, no. 7 (2009): 1583–96. doi:[10.1093/cercor/bhn196](https://doi.org/10.1093/cercor/bhn196)
36. Foster, N. E. V. and Zatorre, R. J. **“Cortical Structure Predicts Success in Performing Musical Transformation Judgments”** *Neuroimage* 53, no. 1 (2010): 26–36. doi:[10.1016/j.neuroimage.2010.06.042](https://doi.org/10.1016/j.neuroimage.2010.06.042)
37. Hudziak, J. J., Albaugh, M. D., Ducharme, S., Karama, S., Spottswood, M., Crehan, E., Evans, A. C., Botteron, K. N., and Brain Development Cooperative Group. **“Cortical Thickness Maturation and Duration of Music Training: Health-Promoting Activities Shape Brain Development”** *J Am Acad Child Adolesc Psychiatry* 53, no. 11 (2014): 1153–61, 1161.e1–2. doi:[10.1016/j.jaac.2014.06.015](https://doi.org/10.1016/j.jaac.2014.06.015)
38. Raine, A., Laufer, W. S., Yang, Y., Narr, K. L., Thompson, P., and Toga, A. W. **“Increased Executive Functioning, Attention, and Cortical Thickness in White-Collar Criminals”** *Hum Brain Mapp* (2011): doi:[10.1002/hbm.21415](https://doi.org/10.1002/hbm.21415)
39. Heim, C. M., Mayberg, H. S., Mletzko, T., Nemeroff, C. B., and Pruessner, J. C. **“Decreased Cortical Representation of Genital Somatosensory Field After Childhood Sexual Abuse”** *Am J Psychiatry* 170, no. 6 (2013): 616–23. doi:[10.1176/appi.ajp.2013.12070950](https://doi.org/10.1176/appi.ajp.2013.12070950)
40. Haier, R. J., Karama, S., Leyba, L., and Jung, R. E. **“MRI Assessment of Cortical Thickness and Functional Activity Changes in Adolescent Girls Following Three Months of Practice on a Visual-Spatial Task”** *BMC Res Notes* 2, (2009): 174. doi:[10.1186/1756-0500-2-174](https://doi.org/10.1186/1756-0500-2-174)
41. Worsley, K. J., Chen, J.-I., Lerch, J., and Evans, A. C. **“Comparing Functional Connectivity via Thresholding Correlations and Singular Value Decomposition”** *Philos Trans R Soc Lond B Biol Sci* 360, no. 1457 (2005): 913–20. doi:[10.1098/rstb.2005.1637](https://doi.org/10.1098/rstb.2005.1637)
42. Weiner, M. W., Veitch, D. P., Aisen, P. S., Beckett, L. A., Cairns, N. J., Green, R. C., Harvey, D., Jack, C. R., Jagust, W., Liu, E., Morris, J. C., Petersen, R. C., Saykin, A. J., Schmidt, M. E., Shaw, L., Siuciak, J. A., Soares, H., Toga, A. W., Trojanowski, J. Q., and, Alzheimer’s Disease Neuroimaging Initiative. **“The Alzheimer’s Disease Neuroimaging Initiative: A Review of Papers Published Since Its Inception.”** *Alzheimers Dement* 8, no. 1 Suppl (2012): S1–68.
43. Tustison, N. J., Cook, P. A., Klein, A., Song, G., Das, S. R., Duda, J. T., Kandel, B. M., Strien, N. van, Stone, J. R., Gee, J. C., and Avants, B. B. **“Large-Scale Evaluation of ANTs and FreeSurfer Cortical Thickness Measurements”** *Neuroimage* 99, (2014): 166–79. doi:[10.1016/j.neuroimage.2014.05.044](https://doi.org/10.1016/j.neuroimage.2014.05.044)
44. Tustison, N. J., Avants, B. B., Cook, P. A., Zheng, Y., Egan, A., Yushkevich, P. A., and Gee, J. C. **“N4ITK: Improved N3 Bias Correction”** *IEEE Trans Med Imaging* 29, no. 6 (2010): 1310–20. doi:[10.1109/TMI.2010.2046908](https://doi.org/10.1109/TMI.2010.2046908)
45. Avants, B. B., Klein, A., Tustison, N. J., Woo, J., and Gee, J. C. **“Evaluation of an Open-Access, Automated Brain Extraction Method on Multi-Site Multi-Disorder Data”** (2010):
46. Avants, B. B., Tustison, N. J., Wu, J., Cook, P. A., and Gee, J. C. **“An Open Source Multivariate Frame-**

work for n-Tissue Segmentation with Evaluation on Public Data” *Neuroinformatics* 9, no. 4 (2011): 381–400. doi:[10.1007/s12021-011-9109-y](https://doi.org/10.1007/s12021-011-9109-y)

47. Das, S. R., Avants, B. B., Grossman, M., and Gee, J. C. “**Registration Based Cortical Thickness Measurement**” *Neuroimage* 45, no. 3 (2009): 867–79. doi:[10.1016/j.neuroimage.2008.12.016](https://doi.org/10.1016/j.neuroimage.2008.12.016)

48. Klein, A. and Tourville, J. “**101 Labeled Brain Images and a Consistent Human Cortical Labeling Protocol**” *Front Neurosci* 6, (2012): 171. doi:[10.3389/fnins.2012.00171](https://doi.org/10.3389/fnins.2012.00171)

49. Wang, H., Suh, J. W., Das, S. R., Pluta, J. B., Craige, C., and Yushkevich, P. A. “**Multi-Atlas Segmentation with Joint Label Fusion**” *IEEE Trans Pattern Anal Mach Intell* 35, no. 3 (2013): 611–23. doi:[10.1109/TPAMI.2012.143](https://doi.org/10.1109/TPAMI.2012.143)

50. Manjón, J. V., Coupé, P., Martí-Bonmatí, L., Collins, D. L., and Robles, M. “**Adaptive Non-Local Means Denoising of MR Images with Spatially Varying Noise Levels**” *J Magn Reson Imaging* 31, no. 1 (2010): 192–203. doi:[10.1002/jmri.22003](https://doi.org/10.1002/jmri.22003)

51. Lehmann, G. and Legland, D. “**Efficient N-Dimensional Surface Estimation Using Crofton Formula and Run-Length Encoding**” *Insight Journal* (2012):

52. Hasan, K. M., Mwangi, B., Cao, B., Keser, Z., Tustison, N. J., Kochunov, P., Frye, R. E., Savatic, M., and Soares, J. “**Entorhinal Cortex Thickness Across the Human Lifespan**” *J Neuroimaging* 26, no. 3 (2016): 278–82. doi:[10.1111/jon.12297](https://doi.org/10.1111/jon.12297)

53. Price, A. R., Bonner, M. F., Peelle, J. E., and Grossman, M. “**Converging Evidence for the Neuroanatomic Basis of Combinatorial Semantics in the Angular Gyrus**” *J Neurosci* 35, no. 7 (2015): 3276–84. doi:[10.1523/JNEUROSCI.3446-14.2015](https://doi.org/10.1523/JNEUROSCI.3446-14.2015)

54. Wisse, L. E. M., Butala, N., Das, S. R., Davatzikos, C., Dickerson, B. C., Vaishnavi, S. N., Yushkevich, P. A., Wolk, D. A., and Alzheimer’s Disease Neuroimaging Initiative. “**Suspected Non-AD Pathology in Mild Cognitive Impairment**” *Neurobiol Aging* 36, no. 12 (2015): 3152–62. doi:[10.1016/j.neurobiolaging.2015.08.029](https://doi.org/10.1016/j.neurobiolaging.2015.08.029)

55. Betancourt, L. M., Avants, B., Farah, M. J., Brodsky, N. L., Wu, J., Ashtari, M., and Hurt, H. “**Effect of Socioeconomic Status (SES) Disparity on Neural Development in Female African-American Infants at Age 1 Month**” *Dev Sci* (2015): doi:[10.1111/desc.12344](https://doi.org/10.1111/desc.12344)

56. Tustison, N. J., Avants, B. B., Cook, P. A., Kim, J., Whyte, J., Gee, J. C., and Stone, J. R. “**Logical Circularity in Voxel-Based Analysis: Normalization Strategy May Induce Statistical Bias**” *Hum Brain Mapp* 35, no. 3 (2014): 745–59. doi:[10.1002/hbm.22211](https://doi.org/10.1002/hbm.22211)

57. Yushkevich, P. A., Avants, B. B., Das, S. R., Pluta, J., Altinay, M., Craige, C., and Alzheimer’s Disease Neuroimaging Initiative. “**Bias in Estimation of Hippocampal Atrophy Using Deformation-Based Morphometry Arises from Asymmetric Global Normalization: An Illustration in ADNI 3 T MRI Data**” *Neuroimage* 50, no. 2 (2010): 434–45. doi:[10.1016/j.neuroimage.2009.12.007](https://doi.org/10.1016/j.neuroimage.2009.12.007)

58. Reuter, M. and Fischl, B. “**Avoiding Asymmetry-Induced Bias in Longitudinal Image Processing**” *Neuroimage* 57, no. 1 (2011): 19–21. doi:[10.1016/j.neuroimage.2011.02.076](https://doi.org/10.1016/j.neuroimage.2011.02.076)

59. Reuter, M., Schmansky, N. J., Rosas, H. D., and Fischl, B. “**Within-Subject Template Esti-**

mation for Unbiased Longitudinal Image Analysis” *Neuroimage* 61, no. 4 (2012): 1402–18. doi:[10.1016/j.neuroimage.2012.02.084](https://doi.org/10.1016/j.neuroimage.2012.02.084)

60. Avants, B. B., Yushkevich, P., Pluta, J., Minkoff, D., Korezykowski, M., Detre, J., and Gee, J. C. “**The Optimal Template Effect in Hippocampus Studies of Diseased Populations**” *Neuroimage* 49, no. 3 (2010): 2457–66. doi:[10.1016/j.neuroimage.2009.09.062](https://doi.org/10.1016/j.neuroimage.2009.09.062)

61. Avants, B. B., Duda, J. T., Kilroy, E., Krasileva, K., Jann, K., Kandel, B. T., Tustison, N. J., Yan, L., Jog, M., Smith, R., Wang, Y., Dapretto, M., and Wang, D. J. J. “**The Pediatric Template of Brain Perfusion**” *Sci Data* 2, (2015): 150003. doi:[10.1038/sdata.2015.3](https://doi.org/10.1038/sdata.2015.3)

62. Bartko, J. J. “**On Various Intraclass Correlation Reliability Coefficients.**” *Psychological bulletin* 83, no. 5 (1976): 762.

63. Carpenter, B., Gelman, A., Hoffman, M., Lee, D., Goodrich, B., Betancourt, M., Brubaker, M. A., Guo, J., Li, P., and Riddell, A. “**Stan: A Probabilistic Programming Language**” *J Stat Softw* (2016):